Planta (2002) 216: 44–56
DOI 10.1007/s00425-002-0866-6

ORIGINAL ARTICLE

Axel Müller · Petra Düchting · Elmar W. Weiler

A multiplex GC-MS/MS technique for the sensitive and quantitative single-run analysis of acidic phytohormones and related compounds, and its application to *Arabidopsis thaliana*

Received: 3 April 2002 / Accepted: 2 July 2002

Abstract A highly sensitive and accurate multiplex gas chromatography–tandem mass spectrometry (GC-MS/MS) technique is reported for indole-3-acetic acid, abscisic acid, jasmonic acid, 12-oxo-phytodienoic acid and salicylic acid. The optimized setup allows the routine processing and analysis of up to 60 plant samples of between 20 and 200 mg of fresh weight per day. The protocol was designed and the equipment used was chosen to facilitate implementation of the method into other laboratories and to provide access to state-of-the-art analytical tools for the acidic phytohormones and related signalling molecules. Whole-plant organ-distribution maps for indole-3-acetic acid, abscisic acid, jasmonic acid, 12-oxo-phytodienoic acid and salicylic acid were generated for *Arabidopsis thaliana* (L.) Heynh. For leaves of *A. thaliana*, a spatial resolution of hormone quantitation down to approximately 2 mm^2 was achieved.

Keywords *Arabidopsis* (phytohormones) · Abscisic acid (GC-MS/MS analysis) · Chemical-ionization tandem mass spectrometry · Indole-3-acetic acid (GC-MS/MS analysis) · Jasmonic acid (GC-MS/MS analysis) · 12-Oxo-phytodienoic acid (GC-MS/MS analysis) · Salicylic acid (GC-MS/MS analysis)

Abbreviations ABA: abscisic acid · CI: chemical ionization · EI: electron-impact ionization · GC-MS/MS: chromatography–tandem mass spectrometry · HPOT: hydroperoxytrienoic acid · IAA: indole-3-acetic acid · JA: jasmonic acid · OPDA: 12-oxo-phytodienoic acid · SA: salicylic acid

Dedicated to Professor Dr. Nikolaus Amrhein, Zurich, on the occasion of his 60th birthday.

A. Müller · P. Düchting · E.W. Weiler (✉)
Lehrstuhl für Pflanzenphysiologie, Fakultät für Biologie,
Ruhr-Universität Bochum, 44780 Bochum, Germany
E-mail: elmar.weiler@ruhr-uni-bochum.de
Fax: +49-234-3214187

Introduction

Phytohormones control almost every aspect of plant life. The cloning of many genes encoding enzymes of phytohormone biosynthesis on the one hand and the identification of a growing number of genes involved in phytohormone signalling on the other hand have fueled rapid advances in understanding how plant hormones act. If any, then the following generalizations can be made: (i) Often, there is a highly local and controlled production of enzymes of phytohormone biosynthesis (and, by inference, also of phytohormone itself). Examples include ethylene biosynthetic enzymes in abscission zones (Ecker and Theologis 1994), gibberellin biosynthetic enzymes in embryos (seeds) or meristems (Yamaguchi et al. 2001), enzymes of jasmonate biosynthesis in pollen and abscission zones (Kubigsteltig et al. 1999), the occurrence of auxin in cambial meristems (Uggla et al. 1996, 1998; Tuominen et al. 1997) or the expression of genes of indole-3-acetic acid (IAA)-producing nitrilases in particular tissues such as developing seeds or lateral root primordia (Vorwerk et al. 2001; Kutz et al. 2002). (ii) Particularly, the analysis of regulatory mutants or of plants with an altered phytohormone production has unveiled an amazing degree of interactions among the phytohormones, including not only well-known textbook interactions such as those among auxins and cytokinins, but also interactions among abscisic acid (ABA) and ethylene (Gazzarrini and McCourt 2001), jasmonates and ethylene (Saniewski and Czapski 1985), brassinolides and jasmonates (Müssig et al. 2000), auxins and ethylene (Yang and Hoffman 1984; Zarembinski and Theologis 1994), ethylene and cytokinin (Cary et al. 1995), gibberellins and auxin (Ross and O'Neill 2001), to name but a few. Rather than conceptualizing the phytohormone system as an array of parallel routes of signal processing, this system is more appropriately described as a network of interactions, where changes in a particular segment propagate adjustments in many other areas. Such a

regulatory network has the advantage that many more regulatory inputs, e.g. from environmental stimuli, can be managed and a more flexible fine-tuning of responses is possible.

In stark contrast to how the phytohormones act – highly locally and interconnected – is the way phytohormones are analyzed. Current methodology is focussed largely on a single hormone at a time and is often too cumbersome and frequently too insensitive to be useful for the local analysis of a hormone in a plant tissue or organ. Consequently, only a few such experiments have been carried out in the past, with highlights perhaps being the quantitation of ABA in isolated guard cells of *Vicia faba* (Harris et al. 1988) and the quantitation of IAA in cambial zones of *Pinus sylvestris* (Uggla et al. 1996). These two examples may also serve to illustrate two principal approaches to phytohormone analysis taken during recent years: (i) the use of immunoassays (for review: Weiler 1986) and (ii) the use of mass spectrometry (MS), in most cases coupled to an appropriate separation technique such as high-performance liquid chromatography (HPLC) or gas-chromatography (GC; Edlund et al. 1995; Prinsen et al. 1998). Both technologies allow the determination of trace amounts of organic compounds down to the low picogram (10^{-12} g) or even femtogram (10^{-15} g) range and have their own specific advantages and disadvantages. Perhaps the biggest intrinsic advantage of instrument-based vs. antibody-based methods is the former's capability for multiplex analysis: the analysis of multiple components within the same sample aliquot. And yet, this capability has not been explored in a systematic way for plant hormone analysis despite the fact that such a tool is in urgent need: as mentioned above, it is no longer sufficient in any kind of work involving hormone physiological or developmental biological problems to just focus on one endogenous signal without paying attention to other relevant regulators.

The work reported here provides a readily accessible multiplex technique designed for the simultaneous quantitation of acidic phytohormones (IAA and ABA) and related regulators [the octadecanoids jasmonic acid (JA) and 12-oxo-phytodienoic acid (OPDA), and salicylic acid (SA)] at very high overall sensitivity and suitable for small to very small samples of tissue. The method uses a combination of (i) microscale solid-phase extraction with a minimum number of handling steps and suitability for automation, and (ii) gas chromatography–tandem mass spectrometry (GC-MS/MS) with runtime parameter optimization to ensure maximum selectivity and sensitivity. The use of an ion-trap instrument, which provides full-scan spectra at all detection levels, ensures maximum mass-fragment information to aid unambiguous identification of all compounds at an affordable price. The simultaneous use of heavy-isotope-labelled internal standards for all stages of the procedure and for all compounds to be analyzed ensures fully quantitative and highly reproducible results. The usefulness of the novel technique was demonstrated in creating organ-distribution maps for the levels of several phytohormones in *Arabidopsis thaliana* at the flowering stage.

Materials and methods

Plant material

All work was carried out with the C24-strain of *Arabidopsis thaliana* (L.) Heynh. (seeds originally provided by L. Willmitzer, Golm, Germany). Plants were grown from seeds in standard soil mixed with sand (2:1, v/v) for 2 weeks in a phytotron chamber [8 h photoperiod, 18 °C night temperature, 22 °C day temperature, 180–240 μmol photons m^{-2} s^{-1} of photosynthetically active radiation (PAR) from Osram HQIE Power Star lamps, 70% relative humidity]. Two-week-old seedlings were transferred to fresh soil and planted in rows at a distance of 5–6 cm between plants (28 plants in a 28 cm×46 cm tray). Further growth until harvest at the flowering/fruiting stage took place in a greenhouse with average day temperatures from 22 to 24 °C, average night temperatures from 18 to 20 °C, a relative humidity of 60 ± 10%, and no less than 150 μmol photons m^{-2} s^{-1} PAR (supplementary light, if required, from sodium-vapor lamps). Plants were raised in short days (12 h photoperiod) for another 2–3 weeks until rosettes were fully expanded (5–7 cm diameter) and then transferred to long days (16 h photoperiod) until harvest.

Harvest and extraction of plant material

The desired parts of plants selected for a typical stature and free from any signs of damage or senescence were cut off with a small pair of scissors and immediately transferred into an Eppendorf cup containing 1–1.5 ml methanol and including 10 pmol of each internal standard ($[^2H]_4$-SA, $[^{13}C]_2$-JA, $[^2H]_2$-IAA (Campro Scientific, Berlin, Germany), $[^2H]_6$-ABA, $[^2H]_5$-OPDA). The methanol was kept at a temperature of 50 °C during harvesting. Depending on the type of tissue, sufficient material was harvested until 20–200 mg of fresh weight (FW) had accumulated. The amount of tissue was calculated by weighing the same number of analogous tissue parts of a duplicate sample, which was not extracted. This procedure was chosen to minimize the time from harvest of a particular tissue fragment to its extraction. Weighing of the tissue prior to extraction required too much time and carried with it the danger of artifactual alterations in the levels of certain analytes, particularly that of JA. Immediately after the collection had been completed, the plant material was ground in the solvent using a vibrating-ball micromill (based on the Retsch MM300 ball mill, modified for microscale applications and purchased from Qiagen, Hilden, Germany). The vibrating ball in the tube was made of stainless steel and had a diameter of 3 mm. Tissue disruption was carried out for 10 min at a vibration frequency of 25 s^{-1}. The homogenized tissue was then allowed to incubate in the solvent for 1 h at room temperature. After centrifugation to remove the particles, the supernatant was decanted, and the solvent was removed in a vacuum centrifuge at 45 °C and 10 mbar (Concentrator 5301; Eppendorf, Hamburg, Germany). The dried residue was dissolved in 30 μl methanol and then, 200 μl diethyl ether was added, followed by agitation in the micromill (2 min, 25 s^{-1}) or ultrasonic treatment (Sonorex RK510S; Bandelin, Berlin, Germany). Any particles were removed by centrifugation, and the sample was then applied to a microscale aminopropyl solid-phase extraction-cartridge.

For the experiment shown in the insert of Fig. 6 (within-leaf distribution of IAA), leaves 1.8 cm in length were cut into square segments of dimensions 1.5 mm×1.5 mm using a block of equally spaced razor blades for dissection. The leaf segments were separately harvested and extracted in the presence of $[^2H]_2$-IAA standard (5 pmol). Each extract was composed of 30 leaf segments of an identical leaf position. The experiment was carried out three times. Thus, each of the square fields in Fig. 6 defines the IAA

content in an area of 2.25 mm^2 averaged from 90 individual leaf segments.

Pre-cleaning of samples by microscale solid-phase extraction

The custom-made cartridge consisted of a diethyl ether-washed, silica-based aminopropyl matrix (Varian, Darmstadt, Germany), gel bed 12 mm×1.5 mm, held in place between two 2.5 mm×1.5 mm non-coated polyolefine filters (Filtrona, Reinbek, Germany) at the tip of a 150 mm×1.5 mm i.d. glass capillary. Each column was preconditioned with the starting solvent. After application of the sample by gravity flow, the microcolumn was washed with 250 µl of $CHCl_3$:2-propanol = 2:1 (v/v), and the hormone fraction was eluted twice with 200 µl diethyl ether containing 2% acetic acid. The combined eluates were taken to dryness in a vacuum centrifuge operated for 1 min at 200 mbar, then for a further min at 10 mbar.

In some cases (generally for *A. thaliana* root tissues and when shoot samples of over 200 mg sample size were to be processed), a second solid-phase extraction step was required. In this case, a diethyl ether-washed polystyrene divinylbenzene copolymer (ENV^+; Separtis, Grenzach-Wyhlen, Switzerland) was used in microcolumns of the same type as those described above, which had been preconditioned with the starting solvent. To re-dissolve the dried sample from the first solid-phase extraction, 50 µl of methanol and then 50 µl of water were added and mixed thoroughly. The sample was then passed through the column by gravity flow. After application of the sample, the column was washed with 250 µl of the same solvent. The bound material was then eluted with diethyl ether containing 2% acetic acid, and the eluates were taken to dryness exactly as described for the first solid-phase extraction step.

Synthesis of [ring-$^2H]_6$-ABA

According to Netting and Lidgard (1999), 0.1 mg (±)-*cis*,*trans*-ABA (A 1049; Sigma Munich, Germany) was dissolved in approx. 1 M NaO[^{2}H] in [$^2H]_2O$ (1.0 ml) and allowed to stand overnight at room temperature. Dilution of the reaction mixture with water, acidification with oxalic acid, extraction with diethyl ether and evaporation of the organic solvent gave [ring-$^2H]_6$-ABA ([3′-^{2}H,5′-$^2H_2$,7′-$^2H_3$]-ABA) which was purified by HPLC (Dynamax D200; Varian) on a Luna C18 column (250 mm×4.6 mm i.d., 5 µm particle size; Phenomenex, Aschaffenburg, Germany) using a linear gradient from 10 to 100% methanol in 0.1 M acetic acid. ABA was monitored at 254 nm. The collected fraction was extracted twice with ethyl acetate, and the combined organic phases were dried by vacuum evaporation in a rotary evaporator. The [ring-$^2H]_6$-labelled ABA was dissolved in methanol and quantified by UV spectroscopy (ϵ_{250} = 28,863 l mol^{-1} cm^{-1}). In order to account for losses of deuterium during the MS/MS process using [ring-$^2H]_6$-labelled ABA, the combined signals of the fragments m/z 233 + m/z 234 were calibrated against the m/z 229 fragment of unlabelled ABA when adjusting the deuterated internal standard ABA for MS/MS analysis.

Synthesis of [3,4,5,6-^{2}H]-SA

According to Pederson and Fitzgerald (1985), 10 g SA (Merck, Darmstadt, Germany) was dissolved in 5 ml [$^2H]_4$-methanol and added dropwise to 5% NaO[^{2}H] (Deutero, Kastellaun, Germany) in [$^2H]_2O$ (30.0 ml; Promochem, Wesel, Germany). NiAl alloy (0.5 g; Lancaster, Mühlheim am Main, Germany) was added slowly and under continuous stirring. The solution was boiled under reflux for about 48 h. After cooling, the reaction was terminated by adding concentrated HCl until pH 2 was reached. The reaction mixture was then extracted twice with diethyl ether, and the organic phase was dried over anhydrous Na_2SO_4. The ether was then removed in a stream of nitrogen, and the reaction product was purified using HPLC (Dynamax D200; Varian) on a Luna C8 column (250 mm×4.6 mm i.d., 5 µm particle size; Phenomenex) in isocratic mode applying a flow rate of 1 ml min^{-1} and water:acetonitrile = 75:25 (v/v, containing 0.2 M acetic acid) as the mobile phase. SA was monitored at 236 nm. The collected fraction was extracted twice with ethyl acetate, and the combined organic phases were dried by vacuum evaporation in a rotary evaporator. [3,4,5,6-^{2}H]-SA was dissolved in methanol and quantified by UV spectroscopy (ϵ_{236} = 7,841 l mol^{-1} cm^{-1}).

Synthesis of racemic [17,17,17,18,18-^{2}H]-*cis*-OPDA

[17,17,17,18,18-^{2}H]-linolenic acid ethyl ester (50 mg; Promochem) was dissolved in 500 µl ethanol and mixed with the same volume of 5 N aqueous KOH. After heating for about 1–2 h at 80 °C and cooling on ice, the pH was adjusted to < 2 with concentrated HCl. Linolenic acid was extracted twice with 3 ml diethyl ether. The efficiency of the hydrolysis was checked by thin-layer chromatography (TCL) on silica gel with the solvent system $CHCl_3$:methanol = 100:1, v/v (linolenic acid ethyl ester: R_f = 0.9; linolenic acid: R_f = 0.27). The organic phase was dried in a stream of nitrogen, the fatty acid re-dissolved in ethanol and added dropwise with stirring into 500 ml of oxygen-saturated 0.1 M sodium borate buffer (pH 10.0) containing 0.5 mM EDTA (4 °C). Soybean lipoxidase (11 mg; EC 1.13.11.12; Type I-S; Sigma L-8383), dissolved in 10 ml of the same buffer, was added and after 10 min at 4 °C with continuous stirring, the reaction was stopped with 85% phosphoric acid until pH < 2 was reached. The reaction mixture was extracted twice with 500 ml diethyl ether, and the combined organic phases were dried over anhydrous Na_2SO_4. The solvent was then removed with a rotary evaporator and the residue was re-dissolved in 1 ml of isohexane:ethyl acetate (60:40, v/v) saturated with 0.5 M formic acid and subjected, in 100-µl aliquots, to HPLC. Separations were carried out with a flow of 1 ml min^{-1} using the same solvent in isocratic mode and Nucleosil 100 (240 mm×4.6 mm i.d., 3 µm particle size, pre-column 5 mm×4 mm i.d.) as stationary phase (Knauer, Berlin, Germany). The fraction eluting from 5–6 min containing [17,17,17,18,18-^{2}H]-13-hydroperoxy-9*Z*,11*E*,15*Z*-octadecatrienoic acid ([17,17,17,18,18-^{2}H]-13-HPOT) was collected. The product proved homogeneous after TLC in the same solvent used for HPLC (R_f = 0.7) and was quantified by spectral analysis in methanol: absorption maximum at 235 nm, ϵ_{235} = 23,000 l mol^{-1} cm^{-1}).

[17,17,17,18,18-^{2}H]-13-HPOT (16 mg), dissolved in 2 ml ethanol was added dropwise to 500 ml of 50 mM potassium phosphate buffer (pH 7.0) containing 15 mg protein of a crude extract from an *Escherichia coli* strain overexpressing allene oxide synthase (Laudert et al. 1997). The reaction mixture was stirred for 2 h at room temperature. The mixture was then extracted twice with 500 ml diethyl ether, and the combined organic phases were dried over anhydrous Na_2SO_4, concentrated to a small volume with a rotary evaporator and finally dried in a stream of nitrogen. [17,17,17,18,18-^{2}H]-*cis*-OPDA was purified as described in Stelmach et al. (1998) using HPLC with *n*-hexane:2-propanol:acetic acid = 98:1.61:0.11 (by vol.) as mobile phase and Zorbax Sil (240 mm×4.6 mm i.d., 5 µm particle size, pre-column 5 mm×4 mm i.d.) as stationary phase (R_t = 19.5 min; spectral analysis in methanol: absorption maximum at 221 nm, ϵ_{221} = 10,700 l mol^{-1} cm^{-1}) with an overall yield of approx. 5–10%, based on linolenic acid (100%).

Synthesis of [$^{13}C]_2$-JA

The synthesis of [$^{13}C]_2$-JA by Michael addition was adapted from the methods of Knöfel and Gross (1988) and Dubs and Stüssi (1978) using diazomethane, [$^{13}C]_2$-malonic acid (Isotec, Miamisburg, USA) and 2-(2′*Z*-pentenyl)-2-cyclopenten-1-one (Firmenich, Geneva, Switzerland)). [$^{13}C]_2$-Malonic acid (1 mmol) was dissolved in 1 ml methanol and converted into the methyl ester by treatment with etheral diazomethane. The solvent was reduced to 0.5 ml in a stream of nitrogen and 0.5 mmol 2-(2′Z-pentenyl)-2-cyclopenten-1-one, as well as 200 µl of 0.2 M sodium methanolate were added. The solution was allowed to react about 1.5 h with stirring at room temperature under a nitrogen atmosphere. The reaction was

stopped with 4 µl glacial acetic acid, and the reaction mixture was taken to dryness in a stream of nitrogen. The dried sample was re-dissolved in 100 µl of water and hydrolyzed at 225 °C for about 18 h in a pressure-stable vessel. After cooling, the vessel was opened and the sample was taken up in 3 ml 0.1 M $NaHCO_3$ and extracted five times with 2 ml each time of chloroform. The combined organic phases were dried with anhydrous Na_2SO_4. The obtained $[^{13}C]_2$-JA methyl ester was hydrolyzed in 0.5 N KOH for about 2 h at 60 °C. After acidification with HCl and extraction with ethyl acetate, $[^{13}C]_2$-JA was purified using isocratic HPLC with *n*-hexane:2-propanol:acetic acid = 100:1.6:0.11 (by vol.) as solvent and Nucleosil 100 (250 mm×4 mm i.d., 3 µm particle size, precolumn 5 mm×4 mm i.d.; Knauer) as stationary phase (flow rate 1.5 ml min^{-1}, $R_t = 10.5$ min). Calibration of the 9*Z*-JA standard was done by comparison of signal intensities to those of unlabelled reference 9*Z*-JA using GC-MS (see below) in order to compensate for the presence of a side product, presumably 9*E*-JA (structure not determined in this work), in the final preparation which could not readily be removed on a preparative scale, but was completely separated from 9*Z*-JA on the analytical GC column connected to the mass spectrometer (see peak 2a in Fig. 3).

Gas chromatography–mass spectrometry

The dried extract fractions containing the acidic phytohormones were re-dissolved in 20 µl methanol, treated with 100 µl ethereal diazomethane and transferred to an autosampler vial [Chromacol 05-CTV(A) 116; Fisher Scientific, Schwerte, Germany]. Ethereal diazomethane, synthesized from N-nitrosomethyl urea, needs to be dried over solid KOH for not less than 1 h prior to use. [Please note: all safety precautions must be followed carefully when handling diazomethane!] Excessive diazomethane and the solvent were removed in a gentle stream of nitrogen, and the methylated sample was then taken up in 7 µl of chloroform. Aliquots of 1 µl of each sample were injected into the GC-MS system for separation and mass fragment analysis using the autosampler quoted below.

All spectra were recorded on a Varian Saturn 2000 ion-trap mass spectrometer connected to a Varian CP-3800 gas chromatograph fitted with a CombiPal autoinjector (Varian, Walnut Creek, Calif., USA).

GC settings

Splitless injection (1 µl), splitter opening 1:100 after 1 min, injector temperature 260 °C; separation on a ZB-50 fused silica capillary column (30 m×0.25 mm i.d., 0.25 µm film thickness; Phenomenex) using He carrier gas at 1 ml min^{-1}; temperature program: 1 min isothermally at 50 °C, linear ramp at a rate of 20 °C min^{-1} to 250 °C, 10 min isothermally at 250 °C; transfer line temperature 260 °C.

MS settings

The mass spectrometer was operated in the CI-MRM mode with methanol as the reactant gas and positive ion detection, set at a maximum reaction time of 128 ms, a maximum ionization time of 2 ms, a scan rate of 0.38 s $scan^{-1}$, a multiplier offset voltage of 300 V, an emission current of 30 µA and the resonant waveform type for MS/MS mode together with a parent-ion selection window of three atomic mass units. Parent-ion selections and excitation amplitudes were segmentally switched within each run to meet changing requirements of each analyte as it eluted in order to provide optimum mass-spectrometric performance for each of the hormones during the analysis (see below). Settings for the endogenous compounds were chosen as follows: SA m/z = 153 $[M+H]^+$, 0.60 V; JA m/z = 225 $[M+H]^+$, 0.50 V; IAA m/z = 190 $[M+H]^+$, 0.50 V; ABA m/z = 261 $[M\text{-}H_2O]^+$, 0.50 V; OPDA m/z = 307 $[M+H]^+$, 0.60 V. A second channel analyzing the isotopically labelled internal standards used identical excitation amplitudes for the following parent ions: $[^2H]_4$-SA m/z = 157 $[M+H]^+$; $[^{13}C]_2$-JA m/z = 227 $[M+H]^+$; $[^2H]_2$-IAA m/z = 192 $[M+H]^+$; $[^2H]_6$-ABA m/z = 267 $[M\text{-}H_2O]^+$; $[^2H]_5$-OPDA m/z = 312 $[M+H]^+$. The amounts of endogenous compounds were calculated from the signal ratios of the unlabelled over the stable isotope-containing mass fragments observed in both analyzing channels.

Results and discussion

General considerations for the methodological layout

The overall procedure as described in *Materials and methods* and depicted in the flow-diagram of Fig. 1 is a combination of (i) multiparallel microscale ball-mill extraction (up to 2×24 samples per run), (ii) multiparallel, instrumentation-independent, solid-phase extraction with the capacity to process the same number of samples at the same time (suitable for automation) and (iii) very sensitive and highly selective compound identification and quantitation using capillary GC coupled to ion-trap mass spectrometry in MS/MS mode. The procedure allows one person to manually process and analyze up to 60 samples within 24 h, the rate-limiting step being the time required for the GC-MS/MS analysis. The procedure given here, although leaving room for further improvements, is the result of a thorough optimization of each individual step and incorporates experience gathered over several years. Only the most relevant general aspects can be discussed in this paper.

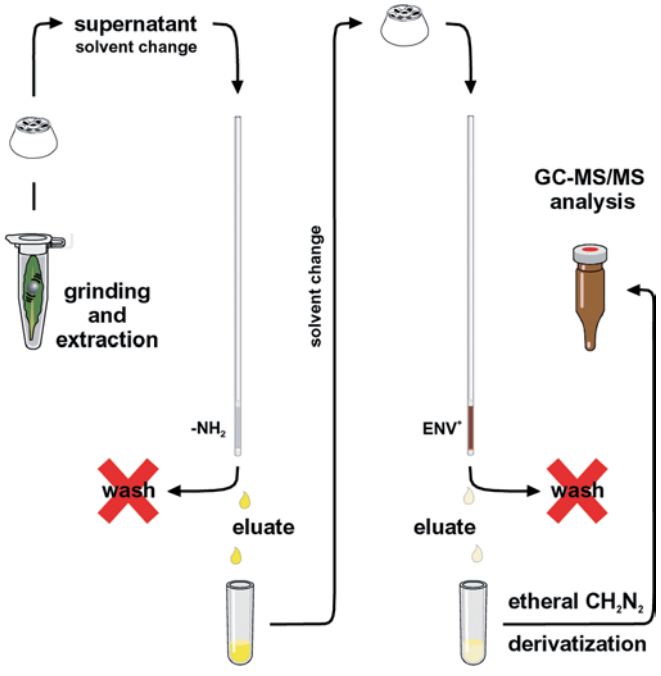

Fig. 1. Flow diagram for the microscale extraction and processing of extracts prior to analysis by gas chromatography–mass spectrometry

Extraction

Undoubtedly, the harvesting and extraction of the plant tissues will critically determine the quality of the results obtained. The hot-methanol extraction used here combines the protein-denaturing power of the hot solvent with rapid penetration of the solvent into the tissue and a high overall solubility of all compounds of interest in the solvent. We have compared the stability of all internal standards during hot-methanol extraction with the conventional extraction using cooled solvents. All recoveries were the same within limits of experimental error (data not shown). Hot methanol has the advantage of giving a better denaturation of endogenous enzymes thus minimizing the danger of artifacts during extraction. One potential problem during sample extraction, when working with *Arabidopsis thaliana* (or other Brassicaceae), is myrosinase-catalyzed degradation of glucosinolates, which results in the release of nitriles (Gmelin and Virtanen 1961; Petersen et al. 2002). This way, indoleacetonitrile is produced and this can lead to erroneous production of IAA from the nitrile precursor. Extraction in hot alcohols circumvents this problem (Gmelin and Virtanen 1961). Multiparallel harvesting of different parts of different organs from the same plants can be done using a 96-well thermoblock compatible with all further workup steps. An alternative would be harvesting in liquid nitrogen. However, this method is less well suited for parallel processing of many small samples. It may be required, though, when very fast changes in analyte levels effected by the workup are a problem. In such cases, we found it preferable to freeze the whole organ (or plant) intact, and then harvest the relevant parts in the frozen state.

Ball-mill extraction using a micro-sample holder, of all the techniques we tried out, emerged as the preferred method as it ensured thorough and uniform extraction of large sets of samples in parallel under exactly the same conditions with no loss of sample.

Extract processing

The layout of this procedural segment was done with the intention of avoiding any step necessitating the sequential handling of the samples, such as HPLC, and to ensure micro-scalability and multiparallel processing capability, using the same format as the milling process. It was also important to preserve compatibility of the method with automatic pipettors/sample processors.

The design of the microscale solid-phase extraction (SPE) columns ensures sufficient sample capacity (see below) and minimizes surface problems which is a point of serious concern when dealing with trace components in small sample volumes. The columns were made from readily available and cheap components (costs approx. 1 Euro per 10 columns). They can be operated at an optimum performance using simple and single-pass free-flow application of the extracts at a flow rate of 25–50 $\mu l\,min^{-1}$. Theoretically, the same range of flow rates can be applied when using the columns in commercial automatic pipetting devices where the samples are drawn into the columns by mild suction and expelled from the columns by mild pressure, allowing double-pass contact of the sample with the matrix and probably yet higher recoveries.

The selection of SPE materials proposed here removes lipids and chlorophyll in the first step. This aminopropyl anion exchanger binds the acidic phytohormones very effectively. For most tissues (e.g. leaves, flowers, fruits and stem tissues of *A. thaliana* and sample sizes up to 100 mg), it has proven unnecessary to follow the aminopropyl column by a second SPE column. However, the two-step procedure was required for root tissue and quantities of shoot tissues larger than 200 mg FW. As the second SPE column, the polystyrene divinylbenzene copolymer ENV^+ was found most appropriate. This matrix binds small molecules according to their lipophilicity but also provides H-bonding capabilities. Its use greatly improves signal-to-noise ratios in cases when the analyte signal is blurred by too much matrix interference after just the first SPE step. In any case, the two-step protocol yields samples of lower matrix load, resulting in less contamination of the GC and the MS system and a longer operational life of the GC columns.

Gas chromatography–mass spectrometry

Modern ion-trap mass spectrometers are robust and, compared to other high-performance mass spectrometers, such as triple-stage quadrupole or sector-field instruments, relatively low-cost instruments of excellent long-term stability of performance and, due to their ion storage capabilities, a high degree of sensitivity. Compound identification is aided, even at lowest analyte levels, by the fact that complete ion spectra are recorded. These are much more informative than the single-ion-monitoring of quadrupole instruments, which is used when operating at the limits of detection. A potential disadvantage of ion traps is the fact that ion intensities change somewhat with the total ion level in the trap, a problem which is not of concern when – as in the procedure reported here – an internal standard is used for each compound to be analyzed and provided the levels

Fig. 2. Mass spectra of unlabelled acidic phytohormones (**a, b**) and heavy isotope-labelled standard compounds (**c**), in each case analyzed as the methyl esters. Electron impact (**a**) and chemical ionization (**b, c**) spectra. The *inserts* in **b** and **c** show the MS/MS daughter-ion spectra, resulting from fragmentation of the base-peak ions selected as parent ions. These are the dominant ions appearing in the CI-MS spectra (corresponding large figures). Each horizontal panel shows the spectra obtained for the hormone drawn on the right of the figure. All ion intensities are given relative to the corresponding base-peak ion (set to 100%). For clarity, scales are drawn only in the graphs of the EI spectra (at right borders)

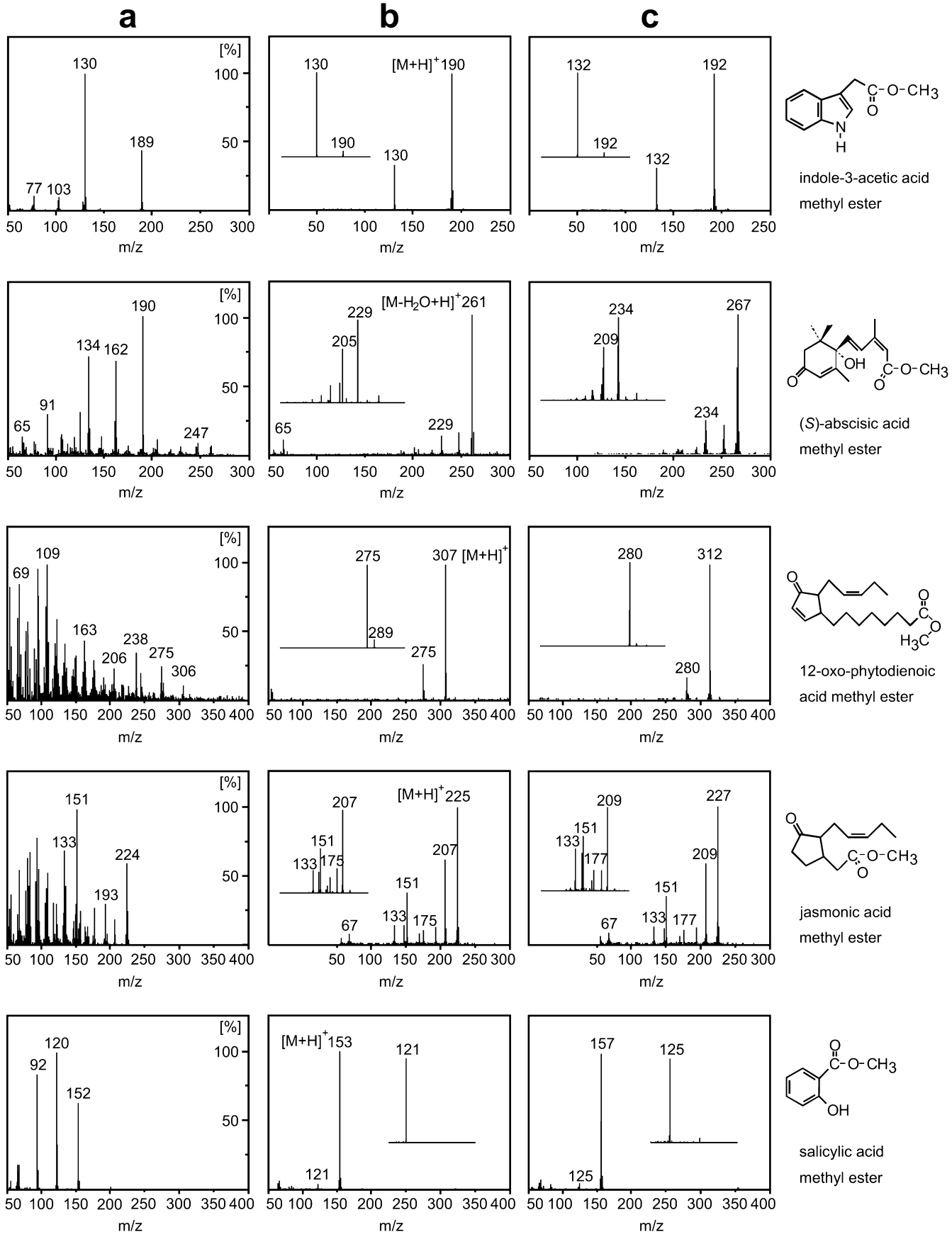
a
b
c
[%]
130
189
77 103
[M+H]+190
190
132
192
m/z
indole-3-acetic acid
methyl ester
190
134 162
91
65
247
[M-H2O+H]+261
229
205
234
267
209
OH
(S)-abscisic acid
methyl ester
109
69
163
238
275
206
306
307 [M+H]+
289
280
312
12-oxo-phytodienoic
acid methyl ester
151
133
224
193
207
175
67
227
jasmonic acid
methyl ester
120
92
152
121
157
125
salicylic acid
methyl ester

of the standard compound added are in the range of the levels of the endogenous compounds to be quantitated. We always determine the optimum level of standard by a preliminary analysis of representative samples in a first run preceding the actual quantitation experiment.

Optimization of sensitivity in the multiplex method reported here required some compromises, mostly related to the nature and level of reactant gas used to generate the parent ions. We found chemical ionization (CI) with methanol as reactant gas the optimum compromise between (i) the efficacy of the ionization process for all compounds of interest as well as for their isotopically labelled standards, and (ii) the requirement for soft fragmentation of the analyte molecules in order to produce parent ion spectra with few fragments of high intensities. Water as the reactant gas would theoretically fragment even more mildly than methanol, but in our hands, the total ion yields were less acceptable. Isobutane, on the other hand, is a more thorough ionizer; however, it also produces more intense fragmentation, which is a disadvantage for MS/MS analysis. As Fig. 2b, c shows, CI with methanol followed by positive-ion detection gave distinct parent-ion spectra allowing characteristic daughter ions to be generated for all compounds of interest from the most intense parent ion. As compared to CI, electron-impact ionization (EI) produced diagnostic spectra, but also severe fragmentation in some cases (e.g., for OPDA and JA), thus limiting the usefulness of the EI mode for the MS/MS multiplex analysis (Fig. 2a).

Thus, in total, the multiplex method described here was designed with the aim of providing high performance for all the plant regulators of interest rather than maximizing performance for a single compound. Consequently, when adapting the technique to monofactorial analysis, there is still much room for further improvements in sensitivity.

Validation of the analytical procedure

As mass spectra obtained in ion-trap instruments may differ somewhat from spectra recorded in quadrupole or sector-field instruments, the complete set of diagnostic reference spectra for all endogenous compounds and all isotopically labelled compounds used as internal standards is given in Fig. 2. The separation of all analytes on the GC column used can be derived from Fig. 3. In this latter figure, the ion intensities of the endogenous compounds as well as the background signals observed are also shown for leaf extracts representing the low (20 mg FW) and the high (200 mg FW) end usually used for further experiments. The lower panel shows the signals of the internal standards against the plant matrix background (for the 200-mg sample only). It is apparent from the figure that even at the low end of the analytical range we define, there are unambiguous signals allowing all analytes to be distinguished from the background with confidence (signal-to-noise ratio >10). The 20-mg sample is equivalent to a single, average-sized leaf of *A. thaliana*. All analytes are baseline-separated from each other including the *cis*- and *trans*-isomers of JA and OPDA, respectively. Although for the purpose of the present study, the sum of the *cis*- and the *trans*-isomers of JA or OPDA has been calculated, the analysis allows routine separate quantitation of the two isomeric forms, of which only the *cis*-form is produced during biosynthesis, whereas the *trans*-form is a result of acid- or base-catalyzed enolization, which leads to accumulation over time in the tissue both during the extraction of the tissue and during the processing of the extracts. Enolization occurs particularly rapidly in the case of JA (Brodschelm 1995), while OPDA enolizes much more slowly.

The reproducibility, sensitivity and accuracy of the overall procedure can be derived from Fig. 4, Fig. 5 and Table 1. For the experiments shown in Fig. 4, dose-response curves were determined using aliquots of extracts each corresponding to 100 mg of fresh weight extracted in 1 ml methanol, for which the endogenous hormone levels had been predetermined by the standard procedure. Different 1-ml aliquots of these extracts were then spiked with different amounts of the appropriate isotopically labelled internal standard, extracts were processed using the two-step SPE procedure and then analyzed by GC-MS/MS. The amount of the added isotopically labelled standard was now calculated for each series of extracts based on the known predetermined amount of endogenous compound, which served as the reference level. The amounts of standard calculated were plotted against the amounts added. It can be seen from Fig. 3 that, in all cases, straight-line relationships with a slope of one within limits of experimental error were obtained, demonstrating the accuracy of the analysis. The small standard deviations of the mean values (see error bars in Fig. 4) show the reproducibility between repetitive experiments that started from different batches of plant material each time and encompassed the sum of all procedural steps. The sensitivity parameters derived from these experiments are listed in Table 1. From the table, for each of the compounds, the minimum detectable amount per GC-injection ($s/n > 10$) and the minimum detectable amount in the samples analyzed (100 mg leaf tissue in 1 ml extract) can be read. Sensitivities are also given as the minimum amounts of tissue to be extracted in order to achieve a fully quantitative determination of the respective hormone. The data show that less than 0.2 mg of tissue would be sufficient to determine OPDA, while the analysis of IAA or JA at the same level of confidence would require 5 or 15 mg of tissue, respectively. Thus, it was decided that, with a safety margin, the multiplex analysis of all five analytes should be carried out with a minimum of 20 mg of tissue (in the case of *A. thaliana* leaf tissue). This is equivalent to a single rosette leaf, see Fig. 3.

The capacity of our microscale procedure was next tested as follows: different amounts of leaf tissue (from

20 to 200 mg) were extracted in the presence of constant amounts of 10 pmol of each of the isotopically labelled internal standards. Extracts were processed using the two-step SPE protocol, and the results (Fig. 5) were plotted as content of analyte vs. amount of tissue extracted. It can be seen that strictly linear relationships exist for all compounds of interest over this whole range of sample sizes. Further experiments (not shown) demonstrated an ample safety margin for the capacity of the procedure for even larger samples (at least up to 500 mg sample fresh weight). However, for all experiments described in the following, care was taken not to exceed the validation limits set by the experiments discussed above. These ranges proved applicable to all tissue types of *A. thaliana* analyzed. We have also demonstrated the applicability of the method for the leaf tissues of maize, barley, rice, tomato and tobacco so far (not shown).

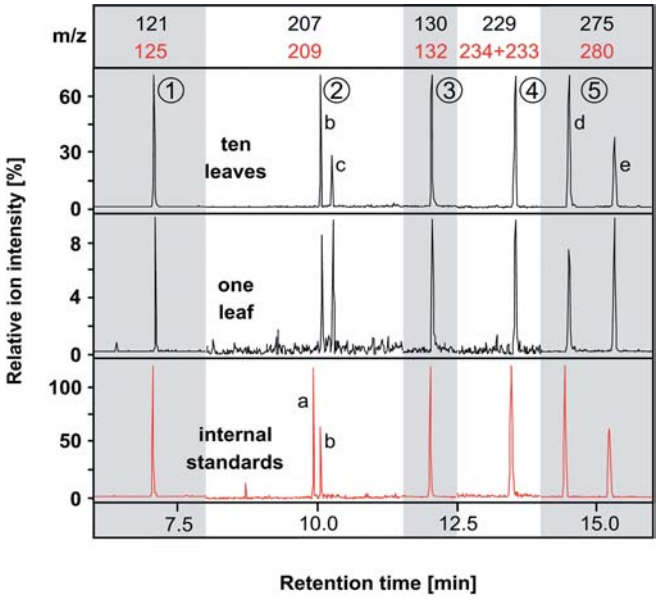

Fig. 3. Typical chromatograms of a multiplex GC-MS/MS hormone analysis of *Arabidopsis thaliana* middle-sized rosette leaves using 20 mg (1 leaf, *middle trace*) or 200 mg (10 leaves, *upper trace*) of tissue from 7- to 8-week-old plants at the flowering stage. The intensities of characteristic daughter-ion fragments selected for each endogenous compound or each internal standard are plotted as one continuous chromatogram. The *grey* and *white* bars indicate the chosen MS/MS-parameter segments and the m/z values in the upper panel indicate the selected mass-to-charge ratios of the daughter-ion mass fragments recorded in the traces below (*black* endogenous compounds, *red* internal standards). SA1 (①) indicated by daughter ion m/z = 121, JA (②) by m/z = 207, IAA (③) by m/z = 130, ABA (④) by m/z = 229, and OPDA (⑤) by m/z = 275. The signals of the internal standards, observed in the 200-mg sample, are shown as an example in the lower (*red*) trace. This trace was constructed from the isotopically labelled daughter ions analogous to those of the endogenous hormones: ($[^2H]_4$-SA, m/z = 125; $[^{13}C]_2$-JA, m/z = 209; $[^2H]_2$-IAA, m/z = 132; $[^2H]_6$-ABA, m/z = 233 + 234; $[^2H]_5$-OPDA, m/z = 280). The *cis*- and *trans*-isomers of JA or OPDA, respectively, gave identical fragment patterns, and the isomers were identified by their differences in retention times. *a*, Presumed unnatural 9*E*-JA present only in the synthetic standard; *b*, *trans*-9*Z*-JA; *c*, *cis*-9*Z*-JA; *d*, *trans*-15*Z*-OPDA; *e*, *cis*-15*Z*-OPDA

Organ-distribution maps for the acidic phytohormones and related regulators in flowering *A. thaliana* plants

In the final series of experiments, the applicability of the multiplex method was demonstrated by generating organ-distribution maps for all regulators of interest for flowering *A. thaliana* plants of a standard habitus: IAA (Fig. 6) and ABA, JA, OPDA as well as SA (Fig. 7). These data provide, for the first time, directly compa-

Fig. 4. Accuracy of the GC-MS/MS analysis of endogenous phytohormones. Rosette leaves of 4- to 5-week-old *A. thaliana* plants were extracted and the extracts were divided into aliquots corresponding to 100 mg FW of tissue (1 ml extract volume). In order to increase the endogenous content of the respective hormones, JA and ABA analyses were carried out using wounded plants (JA) or detached leaves allowed to loose water at room temperature for about 1 h before extraction (ABA). All other plants were harvested without any prior treatment. At the beginning of the extraction, 10 pmol of each internal standard compound was added, and the endogenous amounts of the hormones were quantitatively determined. For the analysis of response ratios, increasing amounts of labelled standard compounds were added to 1-ml aliquots of the extracts, for which the endogenous hormone levels had been predetermined. Extracts were then subjected to the two-stage purification scheme shown in Fig. 1. One-tenth of the final samples, corresponding to a plant matrix contribution from an initial fresh weight of 10 mg leaf material, were then subjected to analysis by GC-MS/MS. The amount of added labelled standard compound found was calculated using the known amounts of the endogenous hormones as the references and plotted against the amount that had in fact been added. Shown are results of $n \geq 5$ independent experiments (average ± SD). R^2, correlation coefficients; the slope of each graph gives the accuracy of the analysis

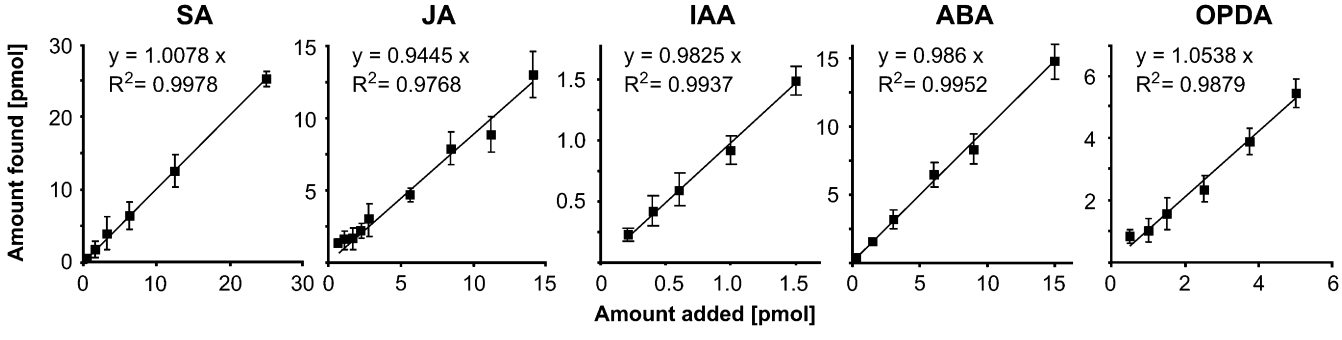

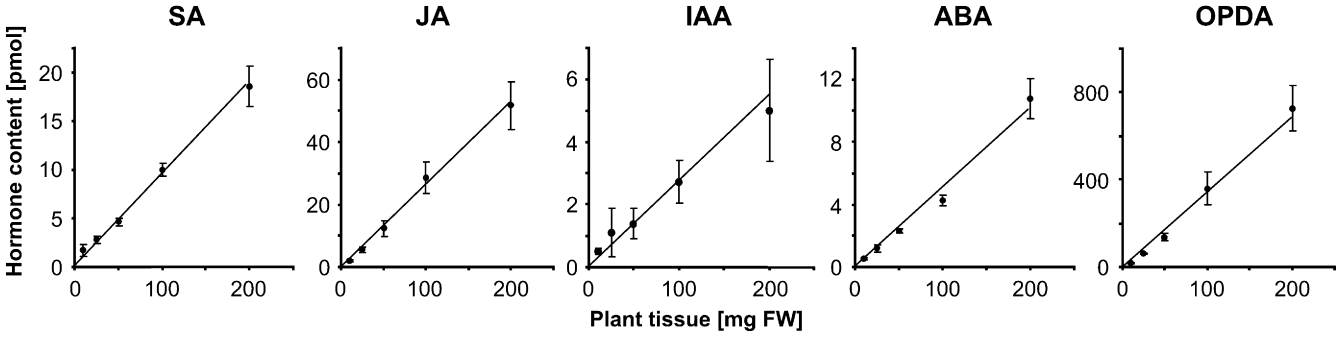

Fig. 5. Capacity of the micro-scale procedure for phytohormone analysis. Different amounts of tissue from rosette leaves of 4- to 5-week-old *A. thaliana* plants were extracted in the presence of 10 pmol of each internal standard. After two-step-purification using aminopropyl- and ENV$^+$-based micro-solid phase extraction (cf. Fig. 1), the samples were subjected to analysis by GC-MS/MS. The amounts of the endogenous metabolites were calculated in relation to the signal of the respective internal standard and are plotted against the amount of tissue analyzed. Shown are results of n≥5 independent experiments (average ± SD)

Table 1. Sensitivity parameters for the GC-MS/MS analysis. The parameters were derived from the analysis of *Arabidopsis thaliana* leaf tissue samples, corresponding to 100 mg FW per extract (cf. Fig. 3) and dosed with known amounts of the given internal standards. The endogenous hormone content of this tissue was known from a first-run analysis and served as the internal reference (pmol from 100 mg fresh leaf material: SA 9.8, JA 70, OPDA 350, IAA 2.8, ABA 47.7)

Analyte	Analytical sensitivity detectable per injection		Process sensitivity detectable per ml extract		Minimum tissue requirement
	pmol	pg	pmol	pg	mg
$[^2H]_4$-SA	0.13	18.1	1.5	204	10
$[^{13}C]_2$-JA	0.21	44.1	3.0	630	15
$[^2H]_5$-OPDA	0.01	2.9	0.15	44	< 0.2
$[^2H]_2$-IAA	0.04	7.0	0.5	87	5
$[^2H]_6$-ABA	0.04	9.8	0.5	123	8

rable reference levels for several signalling compounds throughout one and the same plant and derived from the same tissues. Based on such data sets, it should be much safer to draw conclusions in future experiments, when plants are analyzed under physiological conditions deviating from the normal range, or in mutants showing defined genetic defects. These maps, in the future, will become more and more refined, and further compounds of interest will be added with time.

In order to construct these maps, a reference growth stage was defined as shown in Figs. 6 and 7. This stage is characterized by the presence of all organs, including flowers of all developmental stages, and fruits at different stages of development, but without symptoms of senescence (leaf senescence or fruit ripening). The maps are composed from data from a large number of separate experiments. In each experiment, only particular organs, defined as belonging to one 'harvest-group', were harvested and each individual organ was immersed in the appropriate vessel containing hot methanol as quickly as possible. The harvest-groups were the following: 1) Flowers and fruits, 2) flower-/fruit-stalks, 3) main inflorescence stalk, 4) leaves from the main inflorescence stalk, 5) rosette leaves. For the coflorescences, groups 1), 2) and 3) were likewise harvested as separate groups. Except for the particular harvest-group organs, the rest of the plant was discarded to minimize wound effects. Thus, within each harvest-group and experiment, a fresh set of healthy and undamaged plants was used. The different harvest-groups are represented by separate groups of bars in the block diagrams of Figs. 6 and 7 (which depict, for the sake of clarity, data for only the organs of the main inflorescence and the rosette). The individual categories of organs or organ parts harvested are graphically depicted in the left margin of the block-diagrams, too, and are explained in detail in the legend of Fig. 6.

All organ-distribution maps are colour-coded using the same coding and log-scale plots to visualize the data. Thus, maps can be compared directly. Additionally, the distribution of IAA within the fully expanded rosette leaf (1.8 cm in length) is plotted to visualize the degree of resolution that can be achieved. The distribution of IAA is completely symmetrical between the two halves of leaves, as has been determined in previous experiments (data not shown). As all data in Figs. 6 and 7 are fully quantitative, they can be used for further information retrieval, e.g., to calculate precise ratios for each pair of compounds of interest. This goes beyond the scope of the present work and is thus not discussed here. However, the unprocessed maps are also highly informative. For example, the basipetal auxin gradient decreasing from the shoot tip to the base, which has so far been deduced mainly from analyses of diffusible IAA in bioassays (Went and Thimann 1937), is now substantiated by direct, quantitative measurement. However, similar gradients exist for other regulators, particularly for SA and for OPDA, while the levels of JA and ABA decline only a little. Thus, basipetal gradients in stems are not specifically observed only for IAA. Nevertheless, the inflorescence and coflorescence stalks are sites of remarkably high IAA levels, while leaves, even the youngest ones, contain much lower levels of this growth regulator. In the leaves, our data confirm the notion that young, expanding leaves are characterized by a relatively

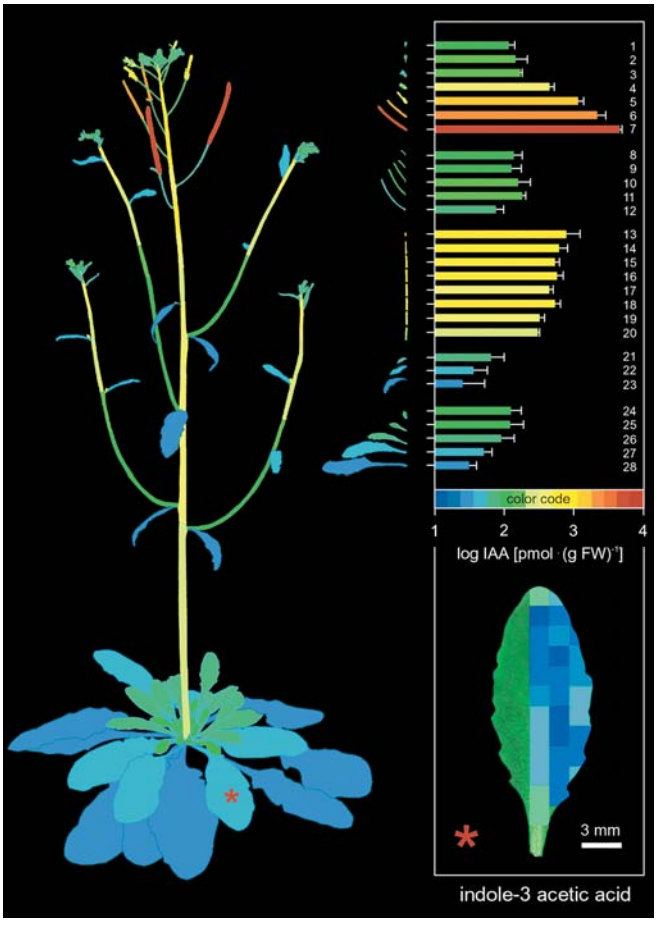

Fig. 6. Organ-distribution map for indole-3-acetic acid. The distribution of IAA levels in the whole *A. thaliana* plant is colour-coded in the drawing. The same colour code applies to the bar diagram which gives the mean values ± SD for the individual plant parts of the main inflorescence stalk and the rosette. The data are based on several independent experiments: Harvest-group 1, flowers and fruits (organ codes *1–7*), $n \geq 5$; harvest group 2, flower and fruit stalks (organ codes *8–12*), $n \geq 3$; harvest group 3, main inflorescence stalk (organ codes *13–20*), $n \geq 3$; harvest group 4, bracts (organ codes *21–23*), $n \geq 10$; harvest group 5, rosette leaves (organ codes *24–28*), $n \geq 10$. The same degree of replication was used for the coflorescence organs. The quantitative colour code also applies to the *insert*, which gives the within-leaf distribution of IAA levels to a resolution of 2.25 mm^2. The organ codes are as follows: *1*, youngest flower buds at the inflorescence tip; *2*, developed, but still closed, flowers at the inflorescence tip; *3*, fully developed flowers at time of anthesis; *4*, 1 day post anthesis (dpa), siliques ca. 3 mm; *5*, 2–3 dpa, siliques ca. 7 mm; *6*, 4–5 dpa, siliques ca. 10 mm; *7*, 6–7 dpa, siliques ca. 15 mm; *8*, flower stalk ca. 3 mm; *9*, flower stalk, ca. 6 mm; *10*, fruit stalk ca. 9 mm; *11*, fruit stalk ca. 13 mm; *12*, fruit stalk ca. 20 mm; *13*, inflorescence stalk top 2 mm; *14*, inflorescence stalk 3–12 mm; *15*, inflorescence stalk 13–22 mm; *16*, inflorescence stalk 23–32 mm; *17*, inflorescence stalk 33–42 mm; *18*, inflorescence stalk 43–52 mm; *19*, inflorescence stalk 53–62 mm; *20*, inflorescence stalk 63–72 mm, *21*, bracts 5–10 mm in length; *22*, bracts, 10–15 mm in length; *23*, bracts >15 mm in length; *24*, rosette leaf ca. 4 mm × <3 mm (length × width), *25*, rosette leaf ca. 8 mm × ca. 4 mm; *26*, rosette leaf ca. 12 mm × ca. 6 mm; *27*, rosette leaf ca. 24 mm × ca. 8 mm; *28*, rosette leaf ca. 36 mm × <10 mm. The * denotes the leaf position for which the IAA distribution is given in the insert

higher IAA level than fully or near fully expanded leaves. Within the leaf, the tip and the margins where the meristematic growth zones are located, are sites of higher IAA levels compared to the central lamina. A very pronounced IAA gradient exists within the central vein area of the leaf with levels of IAA increasing from the tip to the base of the leaf, a situation similar to that reported for young tobacco leaves (Ljung et al. 2001), which may reflect transport of IAA out of the leaf. This process has been related to an inhibition of the development of abscission layers by auxin (Thimann 1977). Alternatively, it may reflect a generally higher auxin level of the vasculature. Auxin has been held responsible for vein differentiation during leaf development (Berleth and Mattsson 2000) and, furthermore, for xylem differentiation in shoots (Thimann 1977; Uggla et al. 1996; Tuominen et al. 1997).

Most remarkable is the strong increase in the level of IAA in flowers starting 1 day after the flowers open and thus concomitantly with the onset of fruit development after pollination. This increase in the level of IAA continues throughout all stages of fruit development analyzed here (which cover all stages of embryo development until early embryo maturation) and can be considered a specific effect, as none of the other compounds analyzed showed a similar increase: levels of SA and JA stayed constant while levels of OPDA declined drastically during fruit development, and levels of ABA showed a transient, but earlier, increase. In contrast to the developing fruits (and also to the inflorescence stalks), the fruit stalks show very low levels of auxin. It is thus likely that the high levels of IAA in developing siliques result from production of the hormone in situ rather than from import into the siliques. Based on the original hypothesis of Nitsch (1953), it has generally been assumed that developing seeds are sites of IAA production required not only for seed (embryo) development, but also for the proliferation of fruit tissues (Thimann 1977). Our data lend strong support for this hypothesis. They are, furthermore, in agreement with the observation that one of the IAA-producing nitrilases, NIT2, is specifically expressed in developing seeds when fruit development begins (Vorwerk et al. 2001). Additionally, developing fruits accumulate high levels of the glucosinolate glucobrassicin (Petersen et al. 2002), which is a precursor of indole-3-acetonitrile, the substrate of nitrilase in the production of IAA. Interestingly, the germination inhibitor ABA reaches its peak level at about the time when IAA levels begin to rise in the developing siliques (compare stages 4 and 5 in Figs. 6 and 7), and its levels decline thereafter against a background of rising levels of IAA. This may be the reason for the very mild dormancy that is observed in seeds of *A. thaliana*.

It is obvious that interpretations of data in Figs. 6 and 7 are greatly aided by the fact that any differential behaviour becomes readily apparent against the body of data for all the other compounds. Monofactorial analysis can never achieve this level of distinction.

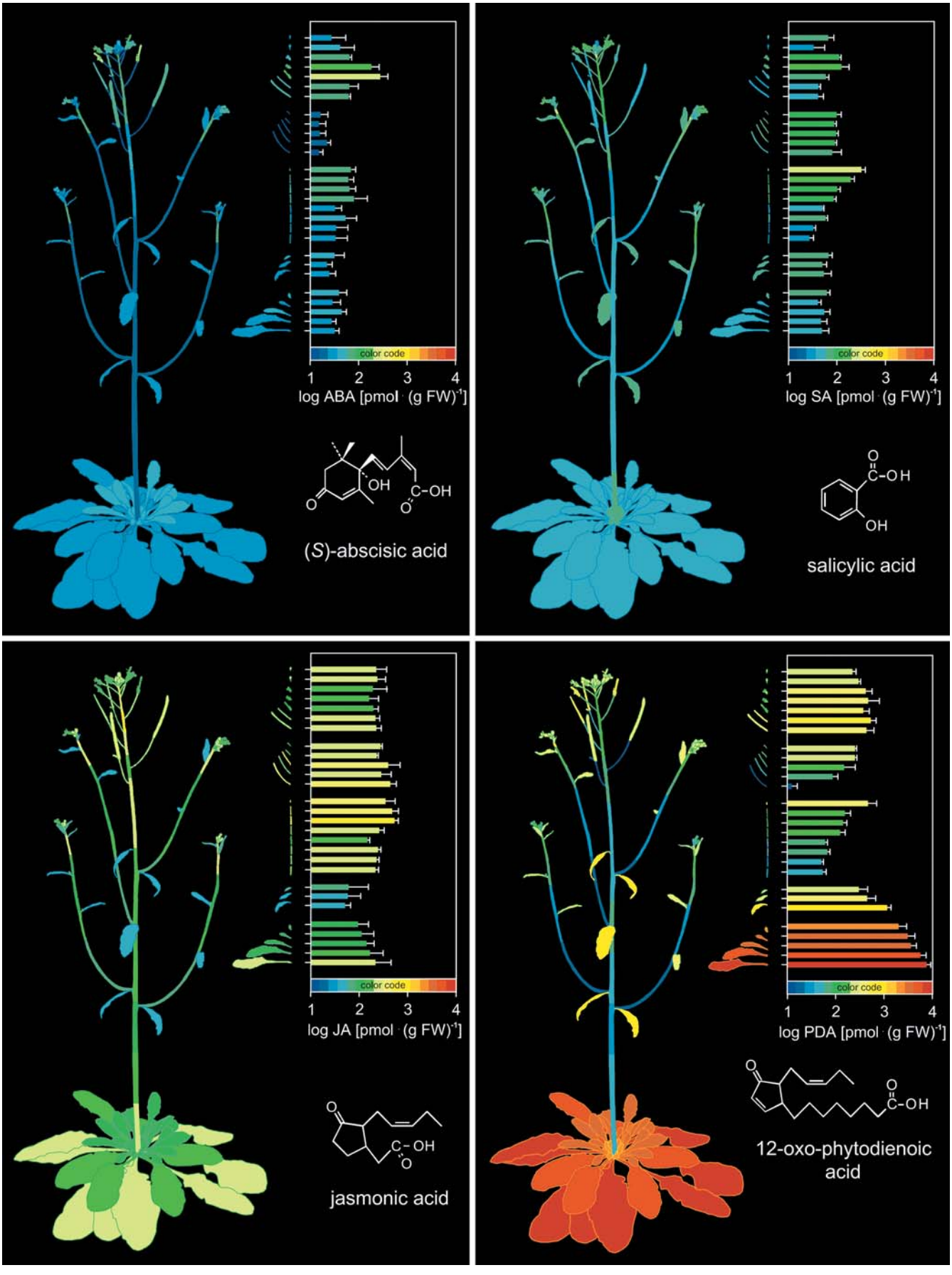
color code
1 2 3 4
log ABA [pmol · (g FW)-1]
OH
C-OH
O
(S)-abscisic acid
log SA [pmol · (g FW)-1]
C-OH
OH
salicylic acid
log JA [pmol · (g FW)-1]
C-OH
jasmonic acid
log PDA [pmol · (g FW)-1]
C-OH
12-oxo-phytodienoic acid

Fig. 7. Organ-distribution maps for ABA, SA, JA and OPDA. All experimental details and parameters are exactly the same as in Fig. 6. For JA and OPDA, the sum of the *cis*- and *trans*-isomers is given

Conclusions

Application of the multiplex GC-MS/MS technique described herein to the analysis of acidic phytohormones and related regulators now allows quantitative data sets about their levels and organ distributions to be obtained at high spatial resolution. The same method is principally applicable to a whole range of other regulators or metabolites of interest. For instance, the gibberellins (methods exemplarily set up in our laboratory for GA_1, GA_4, GA_9 and GA_{20}, using an additional derivatization with trifluoroacetic acid anhydride, which gave excellent fragmentation and sensitivity in the CI-MS/MS mode, data not shown) and further oxylipins, as well as fatty acids, can be analyzed with identical or very similar methodology. The versatility of the technique will be expanded continuously by incorporating further analytes with time. Given the high sensitivity, still finer-resolution maps can be achieved for compounds or organs of interest. For example, it will be possible to analyze the distribution of IAA in seeds and siliques during their development with considerably higher spatial resolution. Furthermore, analyses of changes in the levels of signalling molecules over time can be made at a comparatively high temporal resolution, providing more precise insights into the dynamics of regulatory processes. Most benefit, we believe, will be drawn from the multiplex nature of the analytical process, which minimizes the danger of premature conclusions from simple, monofactorial analyses, which have dominated the field of hormone analysis up to now. This is the best way of acquiring an appreciation of the complex and dynamic interactions of endogenous plant regulators.

Acknowledgement This work was funded by the Deutsche Forschungsgemeinschaft, Bonn (Schwerpunktprogramm 'Molecular Mechanisms of Phytohormone Action') and by Fonds der Chemischen Industrie, Frankfurt/M. (literature provision). The authors thank Firmenich S.A., Geneva, for a generous gift of 2-(2′Z-pentenyl)-2-cyclopenten-1-one.

References

Berleth T, Mattsson J (2000) Vascular development: tracing signals along veins. Curr Opin Plant Biol 3:406–411

Brodschelm W (1995) Untersuchungen zur Jasmonsäure und strukturverwandter Verbindungen als wichtige Signalstoffe im Elicitierungsgeschehen. Dissertation, Munich

Dubs P, Stüssi R (1978) Synthesis of three jasmin constituents via a central intermediate. Helv Chim Acta 61:990–997

Cary AJ, Liu W, Howell SH (1995) Cytokinin action is coupled to ethylene in its effects on the inhibition of root and hypocotyl elongation in *Arabidopsis thaliana* seedlings. Plant Physiol 107:1075–1082

Ecker JR, Theologis A (1994) Ethylene: a unique plant signaling molecule. In: Meyerowitz EM, Somerville CR (eds) *Arabidopsis*. Cold Spring Harbor Laboratory Press, Cold Spring Harbor, NY, pp 485–521

Edlund A, Eklöf S, Sundberg B, Moritz T, Sandberg G (1995) A microscale technique for gas chromatography–mass spectrometry measurements of picogram amounts of indole-3-acetic acid in plant tissues. Plant Physiol 108:1043–1047

Gazzarrini S, McCourt P (2001) Genetic interactions between ABA, ethylene and sugar signaling pathways. Curr Opin Plant Biol 4:387–391

Gmelin R, Virtanen AI (1961) Glucobrassicin, der Precursor von SCN^-, 3-Indolylacetonitril und Ascorbigen in *Brassica oleracea* Species. Ana Acad Sci Fenn Ser A2 107:2–25

Harris MJ, Outlaw WH Jr, Mertens R, Weiler EW (1988) Water-stress-induced changes in the abscisic acid content of guard cells and other cells of *Vicia faba* L. leaves as determined by enzyme-amplified immunoassay. Proc Natl Acad Sci USA 85:2584–2588

Knöfel HD, Gross D (1988) Synthesis of racemic [2-^{14}C]-jasmonic acid. Z Naturforsch Teil C 43:29–31

Kubigsteltig I, Laudert D, Weiler EW (1999) Structure and regulation of the *Arabidopsis thaliana* allene oxide synthase gene. Planta 208:463–471

Kutz A, Müller A, Hennig P, Kaiser WM, Piotrowski M, Weiler EW (2002) A role for nitrilase 3 in the regulation of root morphology in sulphur-starving *Arabidopsis thaliana*. Plant J 30:95–106

Laudert D, Hennig P, Stelmach BA, Müller A, Andert L, Weiler EW (1997) Analysis of 12-oxo-phytodienoic acid enantiomers in biological samples by capillary gas chromatography-mass spectrometry using cyclodextrin stationary phases. Anal Biochem 246:211–217

Ljung K, Bhalero RP, Sandberg G (2001) Sites and homeostatic control of auxin biosynthesis in *Arabidopsis* during vegetative growth. Plant J 28:465–474

Müssig C, Biesgen C, Lisso J, Uwer U, Weiler EW, Altmann T (2000) A novel stress-inducible 12-oxo-phytodienoate reductase from *Arabidopsis thaliana* provides a potential link between brassinosteroid-action and jasmonic-acid synthesis. J Plant Physiol 157:143–152

Netting AG, Lidgard RO (1999) Fragmentation of methyl abscisate and pentafluorobenzyl abscisate in methane electron capture negative ionisation tandem mass spectrometry. J Mass Spectrom 34:611–621

Nitsch JP (1953) Phytohormones et biologie frutière. Fruits 8:91–97

Pedersen AK, Fitzgerald GA (1985) Preparation and analysis of deuterium-labeled Aspirin: application to pharmacokinetic studies. J Pharm Sci 74:188–192

Petersen BL, Chen S, Hansen CH, Olsen CE, Halkier BA (2002) Composition and content of glucosinolates in developing *Arabidopsis thaliana*. Planta 214:562–571

Prinsen E, Van Dongen W, Esmans EL, Van Onckelen HA (1998) Micro and capillary liquid chromatography–tandem mass spectrometry: a new dimension in phytohormone research. J Chromatogr A 826:25–37

Ross J, O'Neill D (2001) New interactions between classical plant hormones. Trends Plant Sci 6:2–3

Saniewski M, Czapski J (1985) Stimulatory effect of methyl jasmonate on ethylene production. Experientia 41:256–257

Stelmach BA, Müller A, Hennig P, Laudert D, Andert L, Weiler EW (1998) Quantitation of the octadecanoid 12-oxo-phytodienoic acid, a signalling compound in plant mechanotransduction. Phytochemistry 47:539–546

Thimann KV (1977) Hormone action in the whole life of plants. The University of Massachusetts Press, Amherst

Tuominen H, Puech L, Fink S, Sundberg B (1997) A radial concentration gradient of indole-3-acetic acid is related to secondary xylem development in hybrid aspen. Plant Physiol 115:577–585

Uggla C, Moritz T, Sandberg G, Sundberg B (1996) Auxin as a positional signal in pattern formation. Proc Natl Acad Sci USA 93:9282–9286

Uggla C, Mellerowicz EJ, Sundberg B (1998) Indole-3-acetic acid controls cambial growth in Scots pine by positional signaling. Plant Physiol 117:113–121

Vorwerk S, Biernacki S, Hillebrand H, Janzik J, Müller A, Weiler EW, Piotrowski M (2001) Enzymatic characterization of the recombinant *Arabidopsis thaliana* nitrilase subfamily encoded by the *NIT*2/*NIT*1/*NIT*3-gene cluster. Planta 212: 508–516

Weiler EW (1986) Plant hormone immunoassays based on monoclonal and polyclonal antibodies. In: Linskens HF, Jackson JF (eds) Modern methods of plant analysis, vol 2. Immunology in plant sciences. Springer, Berlin Heidelberg New York, pp 1–17

Went F, Thimann KV (1937) Phytohormones. MacMillan, New York

Yamaguchi S, Kamiya Y, Sun T (2001) Distinct cell-specific expression patterns of early and late gibberellin biosynthetic genes during *Arabidopsis* seed development. Plant J 28:443–453

Yang SF, Hoffman NE (1984) Ethylene biosynthesis and its regulation in higher plants. Annu Rev Plant Physiol 35:155–189

Zarembinski TI, Theologis A (1994) Ethylene biosynthesis and action: a case of conservation. Plant Mol Biol 26:1579–1597